An algorithm for determining the position of a circle in 3D from its perspective 2D projection.

by Johan Philip

Abstract: We present an algorithm for determining the position of a circle in 3D from its perspective image. The problem has two solutions. The algorithm is based on eigenvalue - eigenvector analysis of a quadratic form associated with the 2D projection.

1. Introduction

The possibility of using photogrammetry for determining the position of a well defined object in an industrial environment has found increasing attention. The boundaries of an object may be known to form a square or rectangle, and this can be used to improve the accuracy of the desciption of the object [6], [7], [8], [9]. Further information is available if the squares and rectangles are known to have vertical or horisontal sides, [11].
In this paper, we consider an object bounded by a circle. An application can be documenting the piping construction inside a nuclear power plant [1], [5]. A flange used for connecting pipes is an easily recognisable circular object. We require just one perspective view of part of the circle to be visible for calculating its 3D position. If several views of the same circle are registered, one can use the present method for each of them and then try to find a compromise solution e.g. by ‘bundle adjustment’, [10].

2. Notations and mathematical formulation.

The coordinates of points in R^3 will be denoted $[X\ Y\ Z]^t$. The origin will be the center of perspectivity and $Z = 1$ will be the embedded projective plane so that the perspective image of $[X\ Y\ Z]^t$ has the coordinates $x = X/Z$ and $y = Y/Z$.
Assume that the circle to be determined has radius = 1 and center in the point $\boldsymbol{P}$ and let the plane of the circle have the normal direction $\hat{\boldsymbol{n}}$, where ^ denotes unit length. We shall assume that the Z-coordinate of $\boldsymbol{P}$ exceeds 2 so that the circle is in front of the projective plane. Our aim is to determine $\boldsymbol{P}$ (=three parameters) and $\pm\hat{\boldsymbol{n}}$ (=two parameters) from the knowledge of the perspective coordinates of at least five points on the circle.

Denote these data points $\boldsymbol{p}_i = \begin{bmatrix} x_i \\ y_i \\ 1 \end{bmatrix}$, $1 \le i \le n$, where $n \ge 5$.

Let $\hat{\boldsymbol{e}}_1$ and $\hat{\boldsymbol{e}}_2$ be two orthogonal unit vectors in the circle plane. A parametric representation of the circle (with parameter θ) is given by

$$\boldsymbol{r}(\theta) = \begin{bmatrix} X \\ Y \\ Z \end{bmatrix} = \boldsymbol{P} + \hat{\boldsymbol{e}}_1 \cos\theta + \hat{\boldsymbol{e}}_2 \sin\theta \ , \ \ 0 \le \theta < 2\pi \ . \tag{2.1}$$

The perspective image of the circle is an ellips which may degenerate to a line segment. We postpone the discussion of the degenerate case to section 5 and assume until then, that we have a true ellips. Let the equation of this ellips be

$$c_1 x^2 + c_2 xy + c_3 y^2 + c_4 x + c_5 y + c_6 = 0 \ . \tag{2.2}$$

The first step of our algorithm is to determine the c_i , $1 \le i \le 6$, from the five or more given points on the ellips. Since (2.2) is homogeneous, the c_i can only be determined up to a multiplicative constant. The second step will be calculation of $\boldsymbol{P}$ and $\hat{\boldsymbol{n}}$ from the c_i .

3. Determination of the ellips equation.

An ellips is uniquely determined by five separate points $\boldsymbol{p_i}$. We shall determine a linear combination of the monomes x^2 , xy , y^2 , x , y , and 1 of (2.2) which is zero for all the five given points. The following 6×6-determinant equation obviously is such a linear combination

$$det \begin{bmatrix} x^2 & xy & y^2 & x & y & 1 \\ x_1^2 & x_1 y_1 & y_1^2 & x_1 & y_1 & 1 \\ \cdot & \cdot & \cdot & \cdot & \cdot & \cdot \\ \cdot & \cdot & \cdot & \cdot & \cdot & \cdot \\ \cdot & \cdot & \cdot & \cdot & \cdot & \cdot \\ x_5^2 & x_5 y_5 & y_5^2 & x_5 & y_5 & 1 \end{bmatrix} = 0 \ . \tag{3.1}$$

It follows that the coefficients c_i are the cofactors of the first row of the determinant.

If the perspective coordinates are noisy, it is useful to know more than five points. Knowing $n > 5$ points, we define the deviations

$$d_i = c_1 x_i^2 + c_2 x_i y_i + c_3 y_i^2 + c_4 x_i + c_5 y_i + c_6 , \tag{3.2}$$

The least squares solution is obtained as the c_j minimizing

$$\sum_{i=1}^{n} d_i^2 . \tag{3.3}$$

subject to the normalization $\sum_{j=1}^{6} c_j^2 = 1$. See [3] for a discussion of the fitting procedure and the normalization. The solution of this minimization problem is described in section 6.

4. Determination of the circle position from the c_i.

The perspective coordinates x and y of (2.2) are obtained as $x = X/Z$ and $y = Y/Z$. Inserting these in (2.2) and multiplying through by Z^2 , we obtain an equation which is satisfied by the points on the circle in R^3

$$c_1 X^2 + c_2 XY + c_3 Y^2 + c_4 XZ + c_5 YZ + c_6 Z^2 = 0 . \tag{4.1}$$

Define the symmetric matrix

$$\boldsymbol{Q} = \frac{1}{2} \begin{bmatrix} 2c_1 & c_2 & c_4 \\ c_2 & 2c_3 & c_5 \\ c_4 & c_5 & 2c_6 \end{bmatrix} . \tag{4.2}$$

Since $\boldsymbol{Q}$ is symmetric, there exists an orthogonal matrix $\boldsymbol{H}$ such that

$$\boldsymbol{Q} = \boldsymbol{H}\Lambda\boldsymbol{H}^t \quad \text{where} \quad \Lambda = \begin{bmatrix} \lambda_1 & & \\ & \lambda_2 & \\ & & \lambda_3 \end{bmatrix} , \tag{4.3}$$

and the eigenvalues λ_1 , λ_2 , and λ_3 are real.

In the rotated coordinates defined by

$$\begin{bmatrix} \xi \\ \eta \\ \zeta \end{bmatrix} = \boldsymbol{H}^t \begin{bmatrix} X \\ Y \\ Z \end{bmatrix} , \tag{4.4}$$

the equation (4.1) takes the form

$$\lambda_1 \xi^2 + \lambda_2 \eta^2 + \lambda_3 \zeta^2 = 0 . \tag{4.5}$$

If the three λ_i have the same sign, only the origin satisfies this equation. For (4.5) to be an ellips, one λ_i must have a sign and opposite to the others. If necessary, change the sign of $\boldsymbol{Q}$ and rearrange the columns of $\boldsymbol{H}$ so that

$$\lambda_1 \geq \lambda_2 > 0 > \lambda_3 \ . \tag{4.6}$$

With $\boldsymbol{r} = \left[X\ Y\ Z\right]^t$, equation (4.1) can be written

$$\boldsymbol{r}^t \boldsymbol{Q} \boldsymbol{r} = 0 \ . \tag{4.7}$$

Inserting (2.1) in (4.7) gives

$$\begin{gathered} \boldsymbol{P}^t\boldsymbol{Q}\boldsymbol{P} + 2\boldsymbol{P}^t\boldsymbol{Q}\hat{e}_1\cos\theta + 2\boldsymbol{P}^t\boldsymbol{Q}\hat{\boldsymbol{e}}_2\sin\theta + \hat{e}_1^t\boldsymbol{Q}\hat{\boldsymbol{e}}_1\cos^2\theta + 2\hat{\boldsymbol{e}}_1^t\boldsymbol{Q}\hat{\boldsymbol{e}}_2\cos\theta\sin\theta + \\ + \hat{\boldsymbol{e}}_2^t\boldsymbol{Q}\hat{\boldsymbol{e}}_2\sin^2\theta = 0 \end{gathered} \tag{4.8}$$

Replacing $\sin^2\theta$ by $1 - \cos^2\theta$, we obtain

$$\begin{gathered} \boldsymbol{P}^t\boldsymbol{Q}\boldsymbol{P} + \hat{\boldsymbol{e}}_2^t\boldsymbol{Q}\hat{\boldsymbol{e}}_2 + (\hat{\boldsymbol{e}}_1^t\boldsymbol{Q}\hat{\boldsymbol{e}}_1 - \hat{\boldsymbol{e}}_2^t\boldsymbol{Q}\hat{\boldsymbol{e}}_2)\cos^2\theta + 2\boldsymbol{P}^t\boldsymbol{Q}\hat{\boldsymbol{e}}_1\cos\theta + 2\boldsymbol{P}^t\boldsymbol{Q}\hat{\boldsymbol{e}}_2\sin\theta + \\ + 2\hat{\boldsymbol{e}}_1^t\boldsymbol{Q}\hat{\boldsymbol{e}}_2\cos\theta\sin\theta = 0 \end{gathered} \ . \tag{4.9}$$

For this to hold for all θ , we must have

$$\begin{aligned} \hat{\boldsymbol{e}}_1^t\boldsymbol{Q}\hat{e}_1 &= \hat{\boldsymbol{e}}_2^t\boldsymbol{Q}\hat{\boldsymbol{e}}_2 = -\boldsymbol{P}^t\boldsymbol{Q}\boldsymbol{P} \\ \hat{\boldsymbol{e}}_1^t\boldsymbol{Q}\hat{\boldsymbol{e}}_2 &= \boldsymbol{P}^t\boldsymbol{Q}\hat{\boldsymbol{e}}_1 = \boldsymbol{P}^t\boldsymbol{Q}\hat{\boldsymbol{e}}_2 = 0 \end{aligned} \ . \tag{4.10}$$

Define

$$\hat{\boldsymbol{f}}_1 = \boldsymbol{H}^t\hat{\boldsymbol{e}}_1 \qquad \hat{f}_2 = \boldsymbol{H}^t\hat{\boldsymbol{e}}_2 \ . \tag{4.11}$$

By the orthogonality of $\boldsymbol{H}$, $\hat{\boldsymbol{f}}_1$ and $\hat{\boldsymbol{f}}_2$ are orthogonal unit vectors and we can write two of the relation in (4.10) as

$$\hat{\boldsymbol{f}}_1^t\Lambda\hat{f}_1 = \hat{\boldsymbol{f}}_2^t\Lambda\hat{\boldsymbol{f}}_2 \quad \text{and} \quad \hat{\boldsymbol{f}}_1^t\Lambda\hat{\boldsymbol{f}}_2 = 0 \ . \tag{4.12}$$

Since a stiff rotation of $\hat{\boldsymbol{e}}_1$ and $\hat{\boldsymbol{e}}_2$ around $\hat{\boldsymbol{n}}$ results in the same circle, we can not expect to be able to determine $\hat{\boldsymbol{f}}_1$ and $\hat{\boldsymbol{f}}_2$ uniquely from (4.12) . In fact, we can choose one coordinate of $\hat{\boldsymbol{f}}_1$ and one of $\hat{\boldsymbol{f}}_2$ and still satisfy (4.12) . Using some geometrical intuition, we choose

$$\hat{\boldsymbol{f}}_1 = \frac{1}{\sqrt{2}}\begin{bmatrix}\cos\varphi \\ 1 \\ \sin\varphi\end{bmatrix} \quad \text{and} \quad \hat{\boldsymbol{f}}_2 = \frac{1}{\sqrt{2}}\begin{bmatrix}-\cos\varphi \\ 1 \\ -\sin\varphi\end{bmatrix} , \tag{4.13}$$

where φ is a parameter to be determined. Then, $\hat{\boldsymbol{f}}_1$ and $\hat{\boldsymbol{f}}_2$ are orthogonal unit vectors satisfying $\hat{\boldsymbol{f}}_1^t \Lambda \hat{\boldsymbol{f}}_1 = \hat{\boldsymbol{f}}_2^t \Lambda \hat{\boldsymbol{f}}_2$ and the remaining condition in (4.12) reads

$$-\lambda_1 \cos^2\varphi + \lambda_2 - \lambda_3 \sin^2\varphi = 0 . \tag{4.14}$$

Rearranging, we obtain

$$\cos^2\varphi = \frac{\lambda_2 - \lambda_3}{\lambda_1 - \lambda_3} . \tag{4.15}$$

By (4.6) this ratio of the λ_i is between 0 and 1, so we can compute $\cos\varphi$. We get two values of $\cos\varphi$ and two values of $\sin\varphi$. Since changing signs of both $\cos\varphi$ and $\sin\varphi$ exchanges $\hat{\boldsymbol{f}}_1$ and $\hat{\boldsymbol{f}}_2$, we have two different solutions. Having $\hat{\boldsymbol{f}}_1$ and $\hat{\boldsymbol{f}}_2$ and using the orthogonality of $\boldsymbol{H}$, we get

$$\hat{\boldsymbol{n}} = \hat{\boldsymbol{e}}_1 \times \hat{\boldsymbol{e}}_2 = \boldsymbol{H}\hat{\boldsymbol{f}}_1 \times \boldsymbol{H}\hat{\boldsymbol{f}}_2 = \pm\boldsymbol{H}(\hat{\boldsymbol{f}}_1 \times \hat{\boldsymbol{f}}_2) = \pm\boldsymbol{H}\begin{bmatrix} -\sin\varphi \\ 0 \\ \cos\varphi \end{bmatrix} . \tag{4.16}$$

Instead of calculating $\boldsymbol{P}$ directly, we will try to find $\Pi = \boldsymbol{H}^t\boldsymbol{P}$. By (4.10), we have

$$\boldsymbol{P}^t\boldsymbol{Q}\hat{\boldsymbol{e}}_1 = \Pi^t\Lambda\hat{\boldsymbol{f}}_1 = 0 \qquad \boldsymbol{P}^t\boldsymbol{Q}\hat{\boldsymbol{e}}_2 = \Pi^t\Lambda\hat{\boldsymbol{f}}_2 = 0 , \tag{4.17}$$

so Π is orthogonal to $\Lambda\hat{\boldsymbol{f}}_1$ and $\Lambda\hat{\boldsymbol{f}}_2$. We get

$$\Pi = \kappa\ \Lambda\hat{\boldsymbol{f}}_1 \times \Lambda\hat{\boldsymbol{f}}_2 = \kappa\ \frac{1}{\sqrt{2}}\begin{bmatrix} \lambda_1\cos\varphi \\ \lambda_2 \\ \lambda_3\sin\varphi \end{bmatrix} \times \frac{1}{\sqrt{2}}\begin{bmatrix} -\lambda_1\cos\varphi \\ \lambda_2 \\ -\lambda_3\sin\varphi \end{bmatrix} = \kappa\lambda_2\begin{bmatrix} -\lambda_3\sin\varphi \\ 0 \\ \lambda_1\cos\varphi \end{bmatrix} \tag{4.18}$$

for some constant κ . To determine κ , we insert $\cos^2\varphi$ according to (4.15) into (4.10) and get

$$-\Pi^t\Lambda\Pi = -\boldsymbol{P}^t\boldsymbol{Q}\boldsymbol{P} = \hat{\boldsymbol{e}}_1^t\boldsymbol{Q}\hat{\boldsymbol{e}}_1 = \hat{\boldsymbol{f}}_1^t\Lambda\hat{\boldsymbol{f}}_1 = \frac{\lambda_1\cos^2\varphi + \lambda_2 + \lambda_3\sin^2\varphi}{2} = \lambda_2 . \tag{4.19}$$

Combining (4.18) with (4.19) , we get $\kappa = \pm\dfrac{1}{\lambda_2\sqrt{-\lambda_1\lambda_3}}$. Inserting this κ in (4.18) , we obtain

$$\boldsymbol{P} = \boldsymbol{H}\Pi = \pm\boldsymbol{H}\begin{bmatrix} -\sqrt{-\lambda_3/\lambda_1}\sin\varphi \\ 0 \\ \sqrt{-\lambda_1/\lambda_3}\cos\varphi \end{bmatrix} . \tag{4.20}$$

The sign shall be chosen so that $\boldsymbol{P}$ is in front of the projective plane.

5. Degenarate ellips.

The perspective projection of the circle may degenerate to a line segment. This happens when the vector $\boldsymbol{P}$ pointing out the center of the circle is orthogonal to the normal $\hat{\boldsymbol{n}}$ of the circle plane . Then, this plane is the one passing through the line segment and the origin. If $\boldsymbol{p}_1$ and $\boldsymbol{p}_2$ are two separate points on the line segment, we get

$$\boldsymbol{n} = \boldsymbol{p}_1 \times \boldsymbol{p}_2 . \tag{5.1}$$

To be able to calculate $\boldsymbol{P}$, we must know the end points of the line segment. Let $\boldsymbol{p}_{e1}$ and $\boldsymbol{p}_{e2}$ be these end points. Normalize them to length 1 and denote them $\hat{\boldsymbol{p}}_{e1}$ and $\hat{\boldsymbol{p}}_{e2}$. The vector $\hat{\boldsymbol{p}}_{e1} + \hat{\boldsymbol{p}}_{e2}$ points in the same direction as $\boldsymbol{P}$ and an exercise with similar triangles gives

$$\boldsymbol{P} = \frac{\hat{\boldsymbol{p}}_{e1} + \hat{\boldsymbol{p}}_{e2}}{\sqrt{1 - (\hat{\boldsymbol{p}}_{e1}^t \hat{\boldsymbol{p}}_{e2})^2}} . \tag{5.2}$$

6. Computer implementation.

In the computer implementation, we have used a subroutine for singular value decomposition (SVD), [4], instead of one for calculating eigen-values and eigen-vectors. The SVD decomposition of $\boldsymbol{Q}$ is

$$\boldsymbol{Q} = \boldsymbol{U}\boldsymbol{S}\boldsymbol{V}^t , \tag{6.1}$$

where $\boldsymbol{U}$ and $\boldsymbol{V}$ are orthogonal and $\boldsymbol{S}$ is diagonal with the nonnegative singular values s_1 , s_2 and s_3 along the diagonal. For a symmetric matrix like $\boldsymbol{Q}$, the matrices $\boldsymbol{U}$ and $\boldsymbol{V}$ and $\boldsymbol{H}$ in (4.3) are the same if one disregards the order and the signs of their columns. With proper ordering, we also have $s_i = |\lambda_i|$. The advantage with our SVD algorithm is that it orders the singular values so that $s_1 \geq s_2 \geq s_3 \geq 0$. Having assumed that the circle is in front of the projection plane $Z = 1$, we know that the bigger axis of the ellips $= \sqrt{-\lambda_3/\lambda_2} < 1$. This implies that the ordering of the columns of $\boldsymbol{V}$ is the one defined in (4.6). In this way, we don't have to bother about the ordering and can take $\boldsymbol{H} = \boldsymbol{V}$ and replace (4.15) by

$$\cos^2\varphi = \frac{s_2 + s_3}{s_1 + s_3} . \tag{6.2}$$

The two values of $\cos\varphi$ give the two solutions. The formulas (4.16) and (4.20) are replaced by

$$\hat{\boldsymbol{n}} = \boldsymbol{V}\begin{bmatrix} -\sin\varphi \\ 0 \\ \cos\varphi \end{bmatrix} \qquad \text{and} \qquad \boldsymbol{P} = \pm\boldsymbol{V}\begin{bmatrix} \sqrt{s_3/s_1}\sin\varphi \\ 0 \\ \sqrt{s_1/s_3}\cos\varphi \end{bmatrix} . \tag{6.3}$$

The SVD algorithm is the natural tool for solving the least squares problem (3.3) to get the coefficients c_j of (2.2). The following method can be used for $n \geq 5$ points on the ellips. Form the $n \times 6$ "design"-matrix $\boldsymbol{A}$ having row i equal to

$$x_i^2 \, , \, x_i y_i \, , \, y_i^2 \, , \, x_i \, , \, y_i \, , \, 1 \; . \tag{6.4}$$

Let $\boldsymbol{c}$ be the 6 -vector with the unknown c_j . Then, we have $\sum_{i=1}^{n} d_i^2 = \|\boldsymbol{A}\boldsymbol{c}\|^2$ where $\| \; \|$ is the Euclidean norm. The least squares problem (3.3) can be formulated

$$\min \|\boldsymbol{A}\boldsymbol{c}\| \; \text{ subject to } \|\boldsymbol{c}\| = 1 \; . \tag{6.5}$$

Let the SVD decomposition of $\boldsymbol{A}$ be

$$\boldsymbol{A} = \boldsymbol{L}\Sigma\boldsymbol{M}^t \; . \tag{6.6}$$

We get

$$\min_{\|\boldsymbol{c}\| = 1} \|\boldsymbol{A}\boldsymbol{c}\| = \min_{\|\boldsymbol{c}\| = 1} \left\|\boldsymbol{L}\Sigma\boldsymbol{M}^t\boldsymbol{c}\right\| = \min_{\|\boldsymbol{c}\| = 1} \left\|\Sigma\boldsymbol{M}^t\boldsymbol{c}\right\| = \min_{\|\boldsymbol{y}\| = 1} \|\Sigma\boldsymbol{y}\| = \sigma_6 \; , \tag{6.7}$$

where $\boldsymbol{M}^t\boldsymbol{c} = \boldsymbol{y}$ and the min is attained for $\boldsymbol{y}^t = (0, 0, 0, 0, 0, 1)$. We get

$$\boldsymbol{c} = \boldsymbol{M}\boldsymbol{y} = \text{the last column of } \boldsymbol{M} \; . \tag{6.8}$$

Using the SVD, it is easy to detect any degeneracy in the data. The number of singular values σ_i different from zero gives the number of independent data points. With five data points there is a perfect fit and $\sigma_6 = 0$. If the data points overlap so that one doesn't have five independent points, σ_5 will be zero. It is easy to recognize when the ellips in fact is a line segment because then, σ_3 will be zero. With noisy data, a singular value is never exactly zero. Then, a very small value of the ratio σ_i/σ_{i-1} is an indication of degeneracy.

7. Geometrical interpretation of the singular values s_1 , s_2 , and s_3.

Since $\lambda_1 = s_1$ and $\lambda_2 = s_2$, it follows from (4.5) that the ratio between the larger and the smaller axis of the ellips equals $\sqrt{s_1/s_2}$.
Inserting (6.2) in (6.3) we obtain after some simplification that

$$||\boldsymbol{P}||^2 = 1 - \frac{s_2}{s_1} + \frac{s_2}{s_3} . \tag{7.1}$$

In general, $1 - s_2/s_1$ is small so that $||\boldsymbol{P}|| \approx \sqrt{s_2/s_3}$, giving the interpretation of s_3 .

8. Computational experience.

We have conducted Monte Carlo tests with randomly generated circles and added random noise to the perspective coordinates. The center $\boldsymbol{P}$ was evenly disributed in a cube with side = 4 and center in the point $(0, 0, 10)$. The normal direction $\hat{\boldsymbol{n}}$ was evenly distributed over all directions. The five or more points on the ellips were chosen according to three different plans: (i) evenly spread over the whole ellips, (ii) evenly spread over two thirds of the ellips, (iii) evenly spread over half of the ellips. We believe that an even spread of the points is resonable when the points are chosen by a human operator. For a pipe flange, it is common that a little more than half the flange is visible.
Noise in the form of independent gaussian errors with standard deviation = 0.001 have been added to the projective coordinates x_i and y_i . Since the average size of these coordinates is about 0.1 the relative error is of the order 1 percent.
The results of the test are presented in tables 1-3. The following three error measures are considered:

(1) $\Delta\boldsymbol{n}$ the angle in degrees between the true and calculated circle normal

(2) $\Delta\boldsymbol{P}$ the angle in degrees between the true and calculated vector to the circle center

(3) $\Delta||\boldsymbol{P}||$ the relative error of the distance to the circle center, i.e. $\left| \frac{||\boldsymbol{P}_{calc}||}{||\boldsymbol{P}_{true}||} - 1 \right|$.

Since the error distributions are far from symmetric, we prefer to present the medians of the errors. Every number is based on 2000 tests.

ellips fract.	5	6	8
1	.84	.74	.68
2/3	1.9	1.6	1.3
1/2	5.0	4.0	3.3

Table 1. Medians of $\Delta \boldsymbol{n}$ in degrees for 5, 6, and 8 points on the ellips.

ellips fract.	5	6	8
1	.056	.048	.043
2/3	.18	.15	.11
1/2	.80	.64	.55

Table 2. Medians of $\Delta \boldsymbol{P}$ in degrees for 5, 6, and 8 points on the ellips.

ellips fract.	5	6	8
1	.007	.007	.006
2/3	.020	.018	.014
1/2	.105	.085	.073

Table 3. Medians of $\Delta\|\boldsymbol{P}\|$ for 5, 6, and 8 points on the ellips.

Notice that (1) the vector $\boldsymbol{P}$ to the center of the circle is more accurately determined than the normal direction $\hat{\boldsymbol{n}}$.

(2) the accuracy of $\boldsymbol{P}$ decreases more abruptly than that of $\hat{\boldsymbol{n}}$ when the fraction of the ellips with marked points decreases to 1/2.

We have investigated how the error measures of Tables 1-3 vary with the size of the added gaussian noise and have found an almost linear dependence up to a noise size 20 times as big as that used in the tables.

We have investigated if there exists any relation between the errors occuring in a particular example and the various singular values calculated for this example. The condition number $\kappa_\sigma = \sigma_1/\sigma_6$ will be large if the chosen points on the ellips hardly determine the ellips. A large value of κ_σ is an indication of low accuracy in the result.

We have found a positive covariance between $\Delta \boldsymbol{n}$ and the ratio s_2/s_1 , which by sec. 7 is related to the eccentricity of the ellips. It is reasonable that it is difficult to distinguish a small perturbation of the circle normal when the projection of the circle is close to circular.

We have tried to use the covariances of the three error measures with the "test variables" κ_σ and s_2/s_1 to sort out examples with large errors. First, we calculate the 85 percent quantiles for these two test variables from the whole test. Then, each test in which either of the test variables exceeds the quantile is discarded. We show in Figure 1. the histograms of $\Delta \boldsymbol{P}$ before and after the discarding. The test variables act almost independently, so that almost 30 percent of the tests will be discarded. The discarding is more effective in removing large errors of $\boldsymbol{P}$ than of $\hat{\boldsymbol{n}}$.

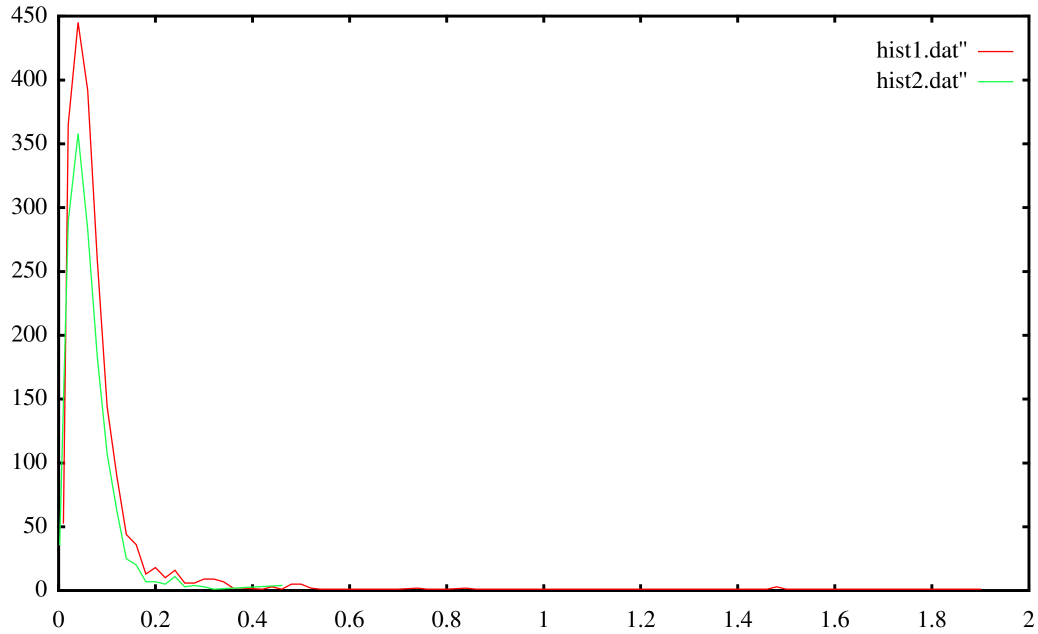

Figure 1. Histograms for $\Delta \boldsymbol{P}$ before and after discarding for an ellips with 5 marked points evenly spread on the whole circumference. The discarding removed 591 tests from the original 2000 tests. That the discarding predominantly removes large errors is manifested in the decrease of the average of $\Delta \boldsymbol{P}$ from .194 to .063 while at the same time the median only decreased from .056 to .052 . Before the discarding the largest error was 1.92 and after .46 .

9. References

[1] K. Andresen and R. Helsch, “Calculation of analytical elements in space using a contour algorithm”, ISPRS Symposium Zurich, Switzerland Sept. 3-7, 1990. SPIE Vol. 1395, Closed-Range Photogrammetry Meets Machine Vision. Eds. A. Gruen and E. Baltsavias.

[2] P. Axelsson, “Autonomous Decisions in Photogrammetry using Minimum Description Length”, TRITA-GEOFOTO Report 1996:11, ISSN 1104-1145.

[3] F.L. Bookstein, “Fitting Conic Sections to Scattered Data”, Computer Graphics and Image Processing (later: Computer Vision, Graphics, and Image Processing) Vol. 9, 1979, pp. 56-71.

[4] G. Golub and C. van Loan, “Matrix Computations”, North Oxford Academic, Oxford 1983.

[5] M.A. Jones, D.P. Chapman, A.A. Hamid and A.T.D. Deacon, “Close range Photogrammetry using Geometric Primitives for efficient CAD modelling of Industrial Plant”, International Archives of Photogrammetry and Remote Sensing, vol. XXXI, part B5, Commission V, Vienna, Austria, 1996, pp. 284-289.

[6] K. Kanatani, The constraints on Images of Rectangular Polyhedra”, IEEE Trans. Patt. Anal.Mach. Intell., vol. PAMI-8, 1986, pp. 456-463

[7] K. Kanatani, “3D Recovery from Angle Clues”, in Proc. 5th Scandinavian Conference on Image Analysis, Stockholm. June 1987, pp. 167-179.

[8] J. Philip, “Motion parameters from right angles”, Journal of Mathematical Imaging and Vision 1, 1992, pp. 107-120.

[9] T. Shakunaga and H. Kaneko, “Perspective Angle Transform and Its Application to 3-D Configuration Recovery”, Prov. IEEE Conference on Computer Vision and Pattern Recognition, Miami Beach, Fl., June 1986, pp. 594-601.

[10]. C. Slama, ed. “Manual of Photogrammetry, Fourth edition”, ISBN 0-937294-01-2, American Society of Photogrammetry, 1980.

[11] H. Zielinski, “Object Reconstruction with Digital Line Photogrammetry”, Photorammetric Report No 61, ISSN 0071-8068, Department of Geodesy and Photogrammetry, Royal Institute of Technology, Stockholm Sweden, 1993.